Multi-physical Modeling and Multi-scale Computation of Nano-Optical Responses

Gang Bao, Guanghui Hu, Di Liu, and Songting Luo

Abstract. We survey recent progresses on multi-physical modeling and multi-scale computation of nano-optical responses. The semi-classical theory treats the evolution of the electromagnetic (EM) field and the motion of the charged particles concurently by coupling Maxwell equations with Quantum Mechanics. A new efficient computational framework is proposed in [**1, 2**] by integrating the Time Dependent Current Density Functional Theory (TD-CDFT). This leads to the coupled Maxwell-Kohn-Sham equations determining the EM field as well as the current and electron densities simultaneously. In the regime of linear responses, a self-consistent multi-scale method is proposed to deal with the well separated space scales. Progresses are also made on developing adaptive Finite Element Methods for the Kohn-Sham equation [**3, 4**].

1. Multi-Physical Modeling and Nano-Optics

The study of optical responses of nano structures has raised a lot of interest in the development of modern physics. When the optical device is of nano scale, the macroscopic theory for the electromagnetic (EM) field based on constitutive relations can not faithfully capture the microscopic and nonlocal characteristics of the light-matter interaction. In this case, it is necessary to consider the quantum mechanical description of the current and charge densities. Quantum Electrodynamics (QED) [**6**] is able to give a complete description of the interactions between photons and electrons. However, the high computational expense prohibits QED from applications. The semi-classical theories [**7, 8, 10**] combine the classical treatment of the EM field and the first principle approach for the charged particles. Different from QED, in a semi-classical theory, the EM field is not quantized and its time evolution is described classically by the Maxwell equations. In the meantime, the motion of charged particles is determined quantum mechanically by Schrödinger equations. To avoid solving the high dimensional many body Schrödinger equation involved in the semi-classical theory, in [**1, 2**], we adopted the Time Dependent Current Density Functional Theory (TD-CDFT) [**18, 19**] to further simplify the model and its computation.

1991 *Mathematics Subject Classification.* 78A45, 81-08, 81V55.

Key words and phrases. Optical response, Nanostructures, Multiscale methods, Adaptive methods, Density Functional Theory.

The research was supported in part by the NSF Focused Research Group grant DMS-0968360.

1.1. The semi-classical theory for nano-optics. The semi-classical theory for nano-optical responses combines classical treatment of the EM field and quantum mechanical description of the charged particles. The evolution of the EM field can be determined by Maxwell equations. In terms of the vector potential $\mathbf{A}$ and scalar potential ϕ, under the Coulomb gauge $\nabla \cdot \mathbf{A} = 0$, the Maxwell equations have the form:

$$\begin{aligned} \frac{1}{c^2}\frac{\partial^2 \mathbf{A}}{\partial t^2} - \nabla^2 \mathbf{A} + \frac{1}{c}\frac{\partial(\nabla\phi)}{\partial t} &= \frac{4\pi}{c}\mathbf{j}, \\ -\nabla^2\phi &= 4\pi\rho, \end{aligned} \tag{1.1}$$

where c is the speed of light in vacuum, and $\mathbf{j}$ and ρ are the current density and charge density related by the continuity equation:

$$\nabla \cdot \mathbf{j} + \frac{\partial \rho}{\partial t} = 0. \tag{1.2}$$

The electric and magnetic fields, $\mathbf{E}$ and $\mathbf{B}$, can be evaluated by

$$\mathbf{E} = -\nabla\phi - \frac{1}{c}\frac{\partial \mathbf{A}}{\partial t}, \qquad \mathbf{B} = \nabla \times \mathbf{A}. \tag{1.3}$$

Notice that in the Maxwell equations, ρ and $\mathbf{j}$ serve as input to compute the EM field. In a classical macroscopic model, they would be determined by the so called constitutive relations as local functions in terms of $\mathbf{E}$ and $\mathbf{B}$. When the size of the sample is of nano scale such that the spatial structure of the resonant states is comparable to or even larger than the wavelength of the light, a microscopic nonlocal treatment must be considered.

Quantum mechanically, the motion of the charged particles is governed by the Schrödinger equation. For a system consisting of N electrons moving under the influence of a given transverse EM field represented by $\mathbf{A}$, the general nonrelativistic Hamiltonian takes the form [**6, 10**]:

$$H_M = \frac{1}{2}\sum_l \left[\mathbf{p}_l + \frac{1}{c}\mathbf{A}(\mathbf{r}_l)\right]^2 + \sum_l v(\mathbf{r}_l) + U, \tag{1.4}$$

where $\mathbf{r}_l$ and $\mathbf{p}_l$ are the coordinate and conjugate momentum of the lth electron, $v(\mathbf{r})$ is the single particle external potential due to the nuclei, and $U = \frac{1}{2}\sum_{l\neq l'} \frac{1}{|\mathbf{r}_l - \mathbf{r}_{l'}|}$ is the mutual Coulomb interaction among electrons. For simplicity, we will assume the Born-Oppenheimer approximation to separate the electronic motion and the nuclear motion for the molecular structures under consideration.

After the incident light is applied, the system will evolve according to the time dependent Schrödinger equation

$$i\frac{\partial \psi(\mathbf{r}_1, ..., \mathbf{r}_N, t)}{\partial t} = H_M \psi(\mathbf{r}_1, ..., \mathbf{r}_N, t). \tag{1.5}$$

The current density $\mathbf{j}(\mathbf{r}, t)$ and electron density $\rho(\mathbf{r}, t)$ can be computed through solutions of (1.5) using

$$\mathbf{j}(\mathbf{r}, t) = < \psi | \hat{\mathbf{j}} | \psi > \quad \text{and} \quad \rho(\mathbf{r}, t) = < \psi | \hat{\rho} | \psi >, \tag{1.6}$$

with the current density operator $\hat{\mathbf{j}}$ and electron density operator $\hat{\rho}$ being given respectively by

$$\begin{aligned} \hat{\mathbf{j}} &= -\frac{1}{2}\sum_l \Big[\mathbf{p}_l\delta(\mathbf{r}-\mathbf{r}_l) + \delta(\mathbf{r}-\mathbf{r}_l)\mathbf{p}_l\Big] - \frac{1}{c}\sum_l \mathbf{A}(\mathbf{r}_l,t), \\ \hat{\rho} &= -\sum_l \delta(\mathbf{r}-\mathbf{r}_l). \end{aligned} \tag{1.7}$$

Notice that in Schrödinger equation (1.5), $\mathbf{A}$ acts as parameters for computing the wavefunction ψ, which will give all physical observables including current and electron densities.

In the semi-classical model, the system is completely described by $(\mathbf{A},\phi)$ and ψ, which affect each other through the coupled Maxwell equations (1.1) and Schrödinger equation (1.5). Therefore they must be determined self-consistently so that equations (1.1) and (1.5) are solved concurrently, which will give rise to the evolution of the EM field and the motion of electrons simultaneously.

1.2. Time dependent current density functional theory. Although the semi-classical theory greatly simplifies the modeling of light-matter interactions at the nano scale, it still poses a significant numerical challenge to solve the high dimensional many body Schrödinger equation involved. Notice that solving the Maxwell equations (1.1) only requires the input of much simpler quantities of the current density $\mathbf{j}$ and electron density ρ. One efficient way to obtain numerical approximations of $(\mathbf{j},\rho)$ is the Time Dependent Current Density Functional Theory (TD-CDFT). The advantage of TD-CDFT is that by restricting to the current and electron densities that are functions of only 3D spatial variables, the computational cost can be greatly reduced.

In TD-CDFT, a system of time dependent Kohn-Sham (KS) equations can be derived in the following form:

$$i\frac{\partial\varphi_l(t)}{\partial t} = H_M^{KS}(t)\varphi_l(t), \tag{1.8}$$

with the following Hamiltonian:

$$H_M^{KS}(t) = \frac{1}{2}\Big[\mathbf{p} + \mathbf{A}_{KS}(\mathbf{r},t)\Big]^2 + v_{KS}(\mathbf{r},t). \tag{1.9}$$

The time dependent KS potential in the above Hamiltonian is given by

$$v_{KS}(\mathbf{r},t) = v(\mathbf{r},t) + v_H(\mathbf{r},t) + v_{xc}(\mathbf{r},t), \tag{1.10}$$

with $v_{xc}(\mathbf{r},t)$ representing the time dependent scalar xc-potential, and

$$\mathbf{A}_{KS}(\mathbf{r},t) = \frac{1}{c}\mathbf{A}(\mathbf{r},t) + \mathbf{A}_{xc}(\mathbf{r},t), \tag{1.11}$$

where $\mathbf{A}$ is the vector potential for the external EM field and $\mathbf{A}_{xc}(\mathbf{r},t)$ is the vector xc-potential. The electron density given and the current density can be given by

$$\rho(\mathbf{r}) = \sum_l f_l|\varphi_l(\mathbf{r})|^2, \tag{1.12}$$

and

$$\mathbf{j}(\mathbf{r},t) = -\frac{i}{2}\sum_l f_l\Big[\varphi_l^*(\mathbf{r},t)\nabla\varphi_l(\mathbf{r},t) - \varphi_l(\mathbf{r},t)\nabla\varphi_l^*(\mathbf{r},t)\Big] + \sum_l f_l|\varphi_l(\mathbf{r})|^2\mathbf{A}_{KS}(\mathbf{r},t), \tag{1.13}$$

where f_l is the occupation number.

1.3. The Maxwell-KS system. We can incorporate the TD-CDFT into the semi-classical theory by replacing the current density and the electron density (1.6) given by solutions of the Schrödinger equation with those obtained by TD-CDFT using (1.12) and (1.13). Therefore the Maxwell equations (1.1) and the time dependent Kohn-Sham equations (1.8) form a coupled system for the EM field ($\mathbf{A}$, ϕ) and the current and electron densities ($\mathbf{j}$, ρ) as they are functionals of each other, i.e.,

$$\begin{cases} (\mathbf{A},\phi) &= \mathcal{M}\big[\mathbf{j},\rho\big]\ ; \\ (\mathbf{j},\rho) &= \mathcal{T}\big[\mathbf{A},\phi\big]\ , \end{cases} \tag{1.14}$$

which suggests that they must be determined self-consistently. From now on, we will refer the above equations as the Maxwell-Kohn-Sham (Maxwell-KS) equations for nano-optics.

For most applications in nano-optics, the induced EM field is varying on a much larger scale than the induced current and electron densities, when the wavelength of the induced EM field is comparable to or larger than the size of the nano structure. Numerically, the mesh size required for the accuracy and stability of solving the Maxwell equations is much larger than the domain we need to handle with TD-CDFT. As a consequence, the coupled Maxwell-KS system can be very ill-conditioned after direct space discretization.

2. Linear Response Theory

The linear response of the Maxwell-KS system (1.14) will further facilitate the computation. In the regime of linear responses, the self-consistent calculation of $(\mathbf{A},\phi)$ and $(\mathbf{j},\rho)$ results in a simple linear system of equations that will allow us to work in the frequency domain.

2.1. Linearized Maxwell-KS system. Rewriting Maxwell equations in the integral form through Green functions shows that the EM field is actually linear functionals of the electron and current densities. On the other hand, the linear response theory of TD-CDFT [**20, 21, 24**] describes the linear relation between the input of the EM field and the output of the microscopic quantities. Combining both theories will lead to the following linear system for the induced EM field ($\delta\mathbf{A}$,

$\delta\phi$) and the induced electron and current densities ($\delta\mathbf{j}$, $\delta\rho$):

$$
\left\{
\begin{array}{rcl}
\delta\mathbf{A}(\mathbf{r},\omega) &=& -\dfrac{1}{c}\displaystyle\int \mathbf{G}(\mathbf{r}-\mathbf{r}')\delta\mathbf{j}(\mathbf{r}')d\mathbf{r}', \\
\delta\phi(\mathbf{r},\omega) &=& -\displaystyle\int \frac{\delta\rho(\mathbf{r}')}{|\mathbf{r}-\mathbf{r}'|}d\mathbf{r}', \\
\delta\mathbf{j}(\mathbf{r},\omega) &=& \displaystyle\int \Big(\chi_{jj}(\mathbf{r},\mathbf{r}',\omega)-\chi_{jj}(\mathbf{r},\mathbf{r}',0)\Big)\cdot\delta\mathbf{A}_{KS}(\mathbf{r}',\omega)d\mathbf{r}' \\
&& \qquad\qquad + \displaystyle\int \chi_{j\rho}(\mathbf{r},\mathbf{r}',\omega)\delta v_{KS}(\mathbf{r}',\omega)d\mathbf{r}', \\
\delta\rho(\mathbf{r},\omega) &=& \displaystyle\int \chi_{\rho j}(\mathbf{r},\mathbf{r}',\omega)\cdot\delta\mathbf{A}_{KS}(\mathbf{r}',\omega)d\mathbf{r}' \\
&& \qquad\qquad + \displaystyle\int \chi_{\rho\rho}(\mathbf{r},\mathbf{r}',\omega)\delta v_{KS}(\mathbf{r}',\omega)d\mathbf{r}',
\end{array}
\right. \tag{2.1}
$$

where the vector and scalar potentials, $\delta\mathbf{A}_{KS}$ and δv_{KS}, are linear functionals in terms of $\delta\mathbf{A}$, $\delta\mathbf{j}$ and $\delta\rho$ such that

$$
\delta\mathbf{A}_{KS}(\mathbf{r},\omega) = \frac{1}{c}(\mathbf{A}_0(\mathbf{r},\omega)+\delta\mathbf{A}(\mathbf{r},\omega)) + \int \mathbf{f}_{xc}(\mathbf{r},\mathbf{r}',\omega)\delta\mathbf{j}(\mathbf{r}',\omega)d\mathbf{r}', \tag{2.2}
$$

and

$$
\delta v_{KS}(\mathbf{r},\omega) = \int \frac{\delta\rho(\mathbf{r}',\omega)}{|\mathbf{r}-\mathbf{r}'|}d\mathbf{r}' + \int f_{xc}(\mathbf{r},\mathbf{r}',\omega)\delta\rho(\mathbf{r}',\omega)d\mathbf{r}', \tag{2.3}
$$

with $\mathbf{f}_{xc} = \delta\mathbf{A}_{xc}/\delta\mathbf{j}$ and $f_{xc} = \delta v_{xc}/\delta\rho$ being the tensor and scalar xc-kernels respectively. Note that ($\delta\mathbf{j}$, $\delta\rho$) in the above equation satisfy the the continuity equation in the frequency domain such that

$$
\delta\rho = \frac{1}{i\omega}\nabla\cdot\delta\mathbf{j}\ . \tag{2.4}
$$

The tensorial Green function $\mathbf{G}$ can be given as

$$
\mathbf{G}(\mathbf{r}-\mathbf{r}') = \frac{e^{iq|\mathbf{r}-\mathbf{r}'|}}{|\mathbf{r}-\mathbf{r}'|}\mathbf{I} + \frac{1}{q^2}\left(\frac{e^{iq|\mathbf{r}-\mathbf{r}'|}}{|\mathbf{r}-\mathbf{r}'|} - \frac{1}{|\mathbf{r}-\mathbf{r}'|}\right)\nabla'\nabla', \tag{2.5}
$$

where $q=\omega/c$ is the wavenumber in vacuum. The linear response function is given by

$$
\begin{aligned}
&\chi_{\alpha\beta}(\mathbf{r},\mathbf{r}',\omega) \\
&= \sum_{ia} f_i\left[\left(\frac{\psi_i(\mathbf{r})\alpha\psi_a(\mathbf{r})\psi_a(\mathbf{r}')\beta\psi_i(\mathbf{r}')}{\epsilon_i-\epsilon_a+\omega}\right) - \left(\frac{\psi_i(\mathbf{r})\alpha\psi_a(\mathbf{r})\psi_a(\mathbf{r}')\beta\psi_i(\mathbf{r}')}{\epsilon_a-\epsilon_i+\omega}\right)^*\right],
\end{aligned} \tag{2.6}
$$

where i and a run over the occupied and unoccupied KS orbitals, respectively. The electron density operator $\boldsymbol{\rho} = 1$ and the following paramagnetic current density operator should be substituted for α and β in (2.6):

$$
\mathbf{j}_p = -i(\nabla-\nabla^\dagger)/2, \tag{2.7}
$$

with $\nabla^\dagger$ acting on all terms to the left.

2.2. P-matrix formulation. To further simply the notations, we choose the following spectral representations for the current and electron densities:

$$\begin{aligned}\delta\mathbf{j}(\mathbf{r},\omega) &= \sum_{ia} f_i \frac{-\omega}{\epsilon_i-\epsilon_a}\psi_i(\mathbf{r})\mathbf{j}_p\psi_a(\mathbf{r})\big[P_{ai}(\omega)-P_{ia}(\omega)\big],\\ \delta\rho(\mathbf{r},\omega) &= \sum_{ia} f_i \psi_i(\mathbf{r})\psi_a(\mathbf{r})\big[P_{ai}(\omega)-P_{ia}(\omega)\big],\end{aligned} \tag{2.8}$$

with the P-matrix elements defined to be

$$\begin{aligned}&P_{ml}(\omega)\\ =&\frac{\dfrac{-\omega}{\epsilon_l-\epsilon_m}\displaystyle\int \psi_m(\mathbf{r})\mathbf{j}_p\psi_l(\mathbf{r})\cdot\delta\mathbf{A}_{KS}(\mathbf{r},\omega)d\mathbf{r}+\int\psi_m(\mathbf{r})\psi_l(\mathbf{r})\delta v_{KS}(\mathbf{r},\omega)d\mathbf{r}}{\epsilon_l-\epsilon_m+\omega},\end{aligned} \tag{2.9}$$

for $\{m,l\}=\{i,a\}$ or $\{a,i\}$. Substituting (2.8) into the first two equations in (2.1) leads to

$$\begin{aligned}\delta\mathbf{A}(\mathbf{r},\omega) &= \sum_{ia} f_i \frac{\omega}{c(\epsilon_i-\epsilon_a)}\\ &\qquad\times\int \mathbf{G}(\mathbf{r}-\mathbf{r}')\psi_i(\mathbf{r}')\mathbf{j}_p\psi_a(\mathbf{r}')d\mathbf{r}'\big[P_{ai}(\omega)-P_{ia}(\omega)\big],\\ \delta\phi(\mathbf{r},\omega) &= \sum_{ia} f_i\int\frac{\psi_i(\mathbf{r}')\psi_a(\mathbf{r}')}{|\mathbf{r}-\mathbf{r}'|}d\mathbf{r}'\big[P_{ai}(\omega)-P_{ia}(\omega)\big].\end{aligned} \tag{2.10}$$

By eliminating ($\mathbf{A}_{KS}$, v_{KS}) and ($\delta\mathbf{j}$, $\delta\rho$) in (2.2)-(2.3), (2.8) and (2.9), we arrive at a linear equation satisfied by the elements of the P-matrix such that for n and n' running over occupied and unoccupied orbitals, we have

$$\begin{aligned}P_{nn'}(\omega)-&\sum_{ia}\frac{K_{nn',ia}(\omega)+M_{nn',ai}(\omega)}{\epsilon_{n'}-\epsilon_n+\omega}P_{ai}(\omega)\\ &+\sum_{ia}\frac{K_{nn',ia}(\omega)+M_{n'n,ia}(\omega)}{\epsilon_{n'}-\epsilon_n+\omega}P_{ia}(\omega)\\ &=\frac{-q}{(\epsilon_{n'}-\epsilon_n+\omega)(\epsilon_{n'}-\epsilon_n)}\int\psi_n(\mathbf{r})\mathbf{j}_p\psi_{n'}(\mathbf{r})\mathbf{A}_0(\mathbf{r},\omega)d\mathbf{r},\\ P_{n'n}(\omega)-&\sum_{ia}\frac{K_{n'n,ai}(\omega)+M_{n'n,ia}(\omega)}{\epsilon_n-\epsilon_{n'}+\omega}P_{ai}(\omega)\\ &+\sum_{ia}\frac{K_{n'n,ai}(\omega)+M_{nn',ai}(\omega)}{\epsilon_n-\epsilon_{n'}+\omega}P_{ia}(\omega).\\ &=\frac{-q}{(\epsilon_n-\epsilon_{n'}+\omega)(\epsilon_n-\epsilon_{n'})}\int\psi_{n'}(\mathbf{r})\mathbf{j}_p\psi_n(\mathbf{r})\mathbf{A}_0(\mathbf{r},\omega)d\mathbf{r},\end{aligned} \tag{2.11}$$

where the coupling matrix $K_{nn',ia}$ is given as

$$\begin{aligned}&K_{nn',ia}(\omega)\\ &=\frac{\omega^2 f_i}{(\epsilon_{n'}-\epsilon_n)(\epsilon_i-\epsilon_a)}\int\psi_n(\mathbf{r})\mathbf{j}_p\psi_{n'}(\mathbf{r})\mathbf{f}_{xc}(\mathbf{r},\mathbf{r}',\omega)\psi_i(\mathbf{r}')\mathbf{j}_p\psi_a(\mathbf{r}')d\mathbf{r}d\mathbf{r}'\\ &\quad+f_i\int\psi_n(\mathbf{r})\psi_{n'}(\mathbf{r})\left(\frac{1}{|\mathbf{r}-\mathbf{r}'|}+f_{xc}(\mathbf{r},\mathbf{r}',\omega)\right)\psi_i(\mathbf{r}')\psi_a(\mathbf{r}')d\mathbf{r}d\mathbf{r}',\end{aligned} \tag{2.12}$$

and the radiative correction $M_{nn',ia}$ has the form:

$$M_{nn',ia}(\omega) = \frac{-\omega^2 f_i}{c^2(\epsilon_n-\epsilon_{n'})(\epsilon_i-\epsilon_a)} \int \psi_n(\mathbf{r})\mathbf{j}_p\psi_{n'}(\mathbf{r})\mathbf{G}(\mathbf{r}-\mathbf{r}')\psi_i(\mathbf{r}')\mathbf{j}_p\psi_a(\mathbf{r}')d\mathbf{r}d\mathbf{r}'. \tag{2.13}$$

The above formulations (2.11) can be put in a compact form for the P-matrix elements:

$$\left[\begin{pmatrix} \mathbf{S} & \mathbf{T} \\ \mathbf{T} & \mathbf{S} \end{pmatrix} - \omega \begin{pmatrix} \mathbf{I} & \mathbf{0} \\ \mathbf{0} & \mathbf{-I} \end{pmatrix}\right] \begin{pmatrix} \mathbf{P} \\ \mathbf{P'} \end{pmatrix} = \begin{pmatrix} \mathbf{F} \\ \mathbf{-F} \end{pmatrix}, \tag{2.14}$$

with

$$\begin{aligned} &\mathbf{P}_{nn'} = P_{nn'}, \mathbf{P'}_{n'n} = P_{n'n}, \\ &\mathbf{S}_{nn',ia} = \delta_{in}\delta_{an'}(\epsilon_i-\epsilon_a) - K_{nn',ia} - M_{nn',ia}, \\ &\mathbf{T}_{nn',ia} = K_{nn',ia} + M_{nn',ia}, \\ &\mathbf{F}_{nn'} = \frac{q}{\epsilon_{n'}-\epsilon_n} \int \psi_n(\mathbf{r})\mathbf{j}_p\psi_{n'}(\mathbf{r})\mathbf{A}_0(\mathbf{r},\omega)d\mathbf{r}. \end{aligned}$$

Furthermore, if we denote $\mathcal{P}_{nn'} = P_{nn'} - P_{n'n}$, then from (2.14) by addition and subtraction, we can get a linear system on $\mathcal{P}_{nn'}$ such that

$$(\mathcal{S} - \omega^2\mathbf{I})\mathcal{P} = \mathcal{F}, \tag{2.15}$$

with

$$\begin{aligned} &\mathcal{S}_{nn',ia} = \delta_{in}\delta_{an'}(\epsilon_i-\epsilon_a)^2 - 2(\epsilon_n-\epsilon_{n'})(K_{nn',ia}+M_{nn',ia}), \\ &\mathcal{F}_{nn'} = 2(\epsilon_n-\epsilon_{n'})\mathbf{F}_{nn'}. \end{aligned} \tag{2.16}$$

The radiative correction $M_{nn',ia}$ is a consequence of the coupling of Maxwell equations and the linear response theory of TD-CDFT. Without the first two equations in (2.1), there will be no $M_{nn',ia}$ in (2.14), which will be reduced to the standard linear response within TD-CDFT [**24**].

2.3. Resonance conditions. Besides the self-consistent determination of the induced EM field and current density, the linear system (2.14) (or equivalently (2.15)) also enables us to determine the resonant eigenmodes of the nano-optical structure. Resonant eigenmodes exist for particular frequencies such that the matrix in (2.14) or (2.15) is degenerate, which are called self-sustaining (SS) modes [**10**]. The resonant structure of optical spectra in general can be determined by the SS modes. Therefore, we can solve

$$\det\left(\begin{pmatrix} \mathbf{S} & \mathbf{T} \\ \mathbf{T} & \mathbf{S} \end{pmatrix} - \omega \begin{pmatrix} \mathbf{I} & \mathbf{0} \\ \mathbf{0} & \mathbf{-I} \end{pmatrix}\right) = 0, \quad \text{or} \quad \det\left(\mathcal{S} - \omega^2\mathbf{I}\right) = 0, \tag{2.17}$$

to determine the eigenfrequencies ω. In particular, we can treat it as an eigenvalue problem to determine the eigenfrequencies ω for the above matrix to have zero eigenvalues.

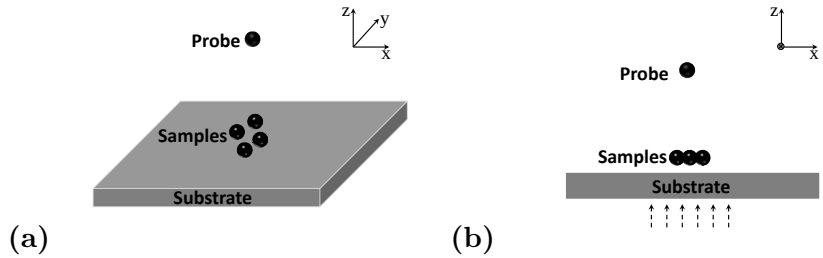

FIGURE 1. SNOM model. (a) model; and (b) example of collection mode: dashed arrows indicate the direction of incident light.

3. The Self-Consistent Multiscale Method

The Maxwell equations are solved on a much larger domain with a coarse grid compared with the smaller domain and a finer grid for TD-CDFT. In order to deal with the multiscale challenge, we propose a multiscale scheme which consists of two solvers: TD-CDFT serving as a **micro solver** $\mathcal{T}_l$ for the current density and the electron density and a **macro solver** $\mathcal{M}_d$ for the Maxwell equations. A self-consistent iteration is adopted to find the solution of the coupled system (2.1), which will lead to the following procedure:

(1) **Micro solver**: at each step indexed by k, with inputs $(\delta\mathbf{A}_k, \delta\phi_k)$, update the induced current and electron densities through the linear response of TD-CDFT, i.e.,

$$(\delta\mathbf{j}_{k+1}, \delta\rho_{k+1}) = \mathcal{T}_l(\delta\mathbf{A}_k, \delta\phi_k),$$

(2) **Macro solver**: with $(\delta\mathbf{j}_{k+1}, \delta\rho_{k+1})$ as fixed parameters, solve the Maxwell equations to update the EM field such that

$$(\delta\mathbf{A}_{k+1}, \delta\phi_{k+1}) = \mathcal{M}_d(\mathbf{j}_{k+1}, \rho_{k+1}),$$

(3) Repeat until a self-consistent solution is reached.

The micro-solver $\mathcal{T}_l$ can be designed to first solve the equation for the P-matrix (2.15) then obtain the current and electron densities through (2.8). Due to the self-consistent structure of the above algorithm, we do not have to pursue an exact solution of (2.15). Instead, a Krylov subspace method will be used to solve (2.15) approximately. For the macro-solver, we can choose a standard scheme such as Finite Difference Method, Finite Element Method, Fast Multipole Method, etc. At each iteration, linear interpolation is used to provide the missing data due to the mismatch between the macro and micro meshes, which essentially allows communications between the macro variable of the EM field and the micro variable of the current and electron densities. The initial EM field $(\delta\mathbf{A}_0, \delta\phi_0)$ can be chosen to be the incident light.

4. Numerical Examples

We present a model calculation of resonant Scanning Near-Field Optical Microscopy (SNOM) as in Figure 1. A substrate supporting the samples is modeled by

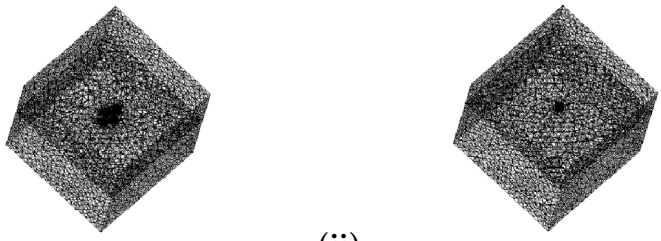

(i) **(ii)**

FIGURE 2. Tetrahedral meshes for solving Maxwell equations: meshes are refined near samples (i) and near probe (ii).

a semi-infinite local dielectric which occupies the half-space $z < 0$. For our numerical experiments, we choose both the samples and the probe as Copper(I) chloride (CuCl). The Maxwell equations are solved with a locally adaptively refined triangular mesh. The ground state occupied and unoccupied KS orbitals are computed with the OCTOPUS package [**26**]. The local density approximation (LDA) and adiabatic local density approximation (ALDA) are used for v_{xc} for ground state and time dependent cases respectively [**27, 28**]. For simplicity, the vector xc-potential $\mathbf{A}_{xc}$ is ignored here.

We first compute the resonant conditions for the model corresponding to different positions of the probe, which is performed by solving the eigenvalue proble as in last section. Table 1 shows the computed lowest eigenvalues. The results show that the position of the probe have very small impact on the resonant conditions. Next we verify our computation of the lowest eigenvalues corresponding to different positions of the probe. The incident field is chosen to be

$$\mathbf{A}_0(\mathbf{r}, \omega) = -ic\mathbf{p} \exp\left(i\omega/c\mathbf{d} \cdot \mathbf{r}\right)/\omega, \tag{4.1}$$

with polarization $\mathbf{p} = (p_x, p_y, p_z)$ and incident direction $\mathbf{d} = (d_x, d_y, d_z)$ such that $||\mathbf{p}|| = 1, ||\mathbf{d}|| = 1$ and $\mathbf{p} \cdot \mathbf{d} = 0$. With this incident field and given frequencies, we solve (2.15) to get the induced current density and the induced EM field. Then we compute the induced dipole moment given as

$$\delta\mu(\omega) = \frac{i}{\omega} \int \delta\mathbf{j}(\mathbf{r}, \omega) d\mathbf{r}. \tag{4.2}$$

TABLE 1. Computed lowest eigenvalues corresponding to different positions of the probe: $s_x = 0nm$, $s_y = 0nm$ or $s_y = 2.6nm$, and $s_z = (2, 3, 4, 5, 6, 7)nm$.

s_z	$3nm$	$4nm$	$5nm$	$6nm$	$7nm$
			$s_y = 2.6nm$		
$\omega(ev)$	3.36761629	3.36759775	3.36761463	3.36757544	3.36761282
			$s_y = 0nm$		
$\omega(ev)$	3.36755793	3.36761002	3.36761394	3.36760513	3.36758880

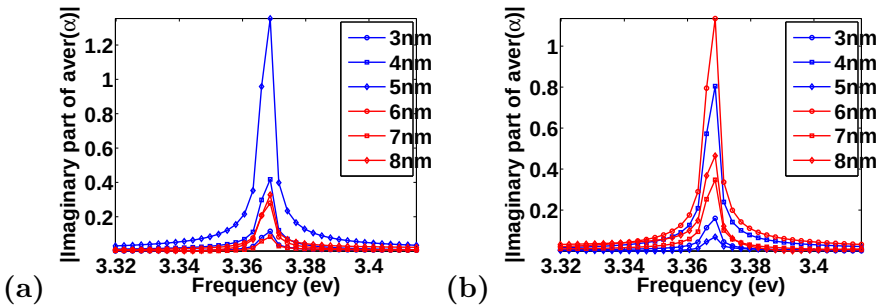

FIGURE 3. Imaginary part of aver(α) corresponding to different position of the probe: (a) $s_x = 0nm$, $s_y = 2.6nm$ and (b) $s_x = 0nm$, $s_y = 0nm$. s_z is indicated in the figure.

The induced dipole moment and the EM field are related through the linear polarizability $\vec{\alpha}$ as

$$\delta\mu = \vec{\alpha}\delta\mathbf{E};\ \vec{\alpha} = \begin{pmatrix} \alpha_{xx} & \alpha_{xy} & \alpha_{xz} \\ \alpha_{yx} & \alpha_{yy} & \alpha_{yz} \\ \alpha_{zx} & \alpha_{zy} & \alpha_{zz} \end{pmatrix}. \tag{4.3}$$

Hence we can compute $\vec{\alpha} = \frac{\delta\mu}{\delta\mathbf{E}}$. In particular, we compute aver(α) $\equiv \frac{\alpha_{xx}+\alpha_{yy}+\alpha_{zz}}{3}$ at the probe. Figure 3 shows the imaginary part of aver(α). We observe a peek at $\omega \approx 3.368(ev)$ which confirms that it is a resonant mode, and the result coincides with the calculation for the eigenvalue value problem (2.17).

5. Adaptive Methods for the Kohn-Sham Equation

5.1. Real-space methods for DFT and TD-DFT. Since their appearance, a lot of work has been devoted to the numerical methods for DFT [**27**] and TDDFT [**28**]. Among those numerical methods, the plane-wave expansion method (PWE) [**13**] is the most popular so far. Despite its successes, the PWE method still has limitations. For example, it is nontrivial to deal with the problem with non-periodic boundary condition, or to implement a parallel version because of the scaling problem. These limitations motivate the development of the real-space methods for the DFT and TDDFT method.

There are several different real-space methods. The finite difference method (FDM) [**9, 17**] is an early one which is used for sloving the Kohn-Sham equation. However, it is not easy to implement the FDM when the computational domain is not regular. In this case, people need to resort to the other numerical methods which can discretize the governing equation on an unstructured mesh. Motivated by this purpose, the numerical methods such as the finite volume method (FVM) [**12**], finite element method (FEM)[**15**], discontinuous Galerkin method (DGM)[**23**], and mesh-free method (MFM)[**22**] have been studied for solving the Kohn-Sham equation.

5.2. The Adaptive Methods for the Kohn-Sham Equation. In [**3, 11**], the h-adaptive method is introduced in solving the Kohn-Sham equation. Unlike the other adaptive methods, the mesh topology is changed after the refinement and/or coarsening. Then an efficient method is necessary to manage the mesh

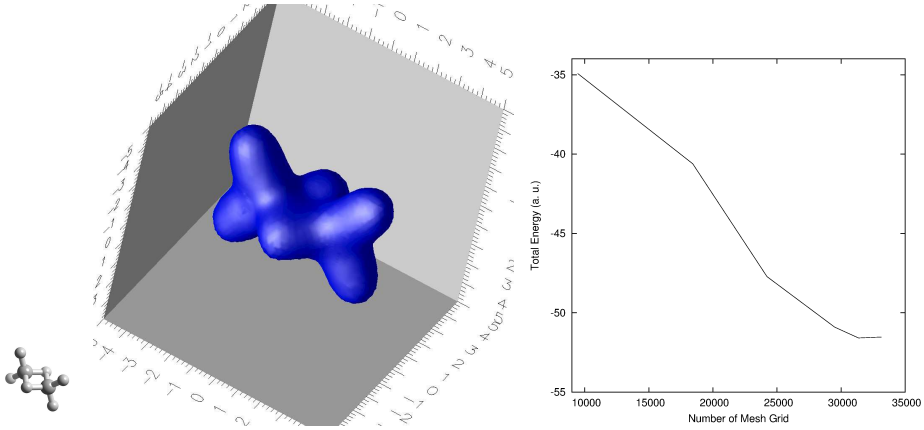

FIGURE 4. Left: The isosurface for a diborane molecule. Right: The convergence curve. In this simulation, the h-adaptive finite element method is used.

data. This is done by using a specific data structure for the mesh grid. For example, a hierarchical geometry tree (HGT) is utilized for this purpose in [**3**]. With HGT, the mesh refinement and/or coarsening can be well-organized, and an efficient interpolation mechanism between two different meshes can also be obtained. A numerical example by h-adaptive method is presented in Fig. 4. In this example, a diborane molecule is simulated. It is observed successfully from the figure that, with the local refinement and/or coarsening of the mesh, the total energy converges to the reference data (-52.628 a. u.). We refer to [**3**] for more numerical examples. In [**14**], an interesting discussion can be found for solving the Kohn-Sham equation by the hp-adaptive method. In this method, besides locally refining and/or coarsening the mesh, the order of the approximate polynomial is also locally enriched.

The r-adaptive method for the Kohn-Sham equation can be found in [**4**]. Different from the h-adaptive method which changes the mesh topology, the r-adaptive method optimizes the distribution of the grid points in the mesh, while keeps the mesh topology unchanged. The general idea is to use a geometry transformation which maps a regular mesh on a domain to a nonuniform mesh on another domain. An early try of the r-adaptive method for the Kohn-Sham equation can be found in [**16**]. To optimize the distribution of the mesh grids, a curvilinear coordinate method is utilized there. By defining a coordinate transformation, a curvilinear grid in the $\vec{x}$-space can be generated from a regular grid in the $\vec{\xi}$-space, and more mesh grids are relocated in the vicinities of the atoms. Another strategy of the mesh redistribution for the Kohn-Sham equation is proposed in [**4**]. Different from the curvilinear coordinate method which explicitly define the map function, the method in [**4**] uses a harmonic map which is generated by solving the following elliptic problem

$$\begin{cases} \nabla_{\vec{x}}(M\nabla_{\vec{x}}\vec{\xi}) &= 0, \\ \vec{\xi}|_{\partial\Omega} &= 0, \end{cases} \tag{5.1}$$

where M is the monitor function which partially controls the movement of the mesh grids. With proper monitor function, the above map $\vec{\xi}(\vec{x})$ can also optimize the distribution of the mesh grids in the vicinities of the atoms. Compared with the curvilinear coordinate method, the strategy with the harmonic maps can totally separate solving PDEs and redistributing the mesh grids, which makes the code reuse for the mesh redistribution possible. We refer to [**4**] for numerical examples by the r-adaptive method.

6. Conclusion and Future Work

To study the response of a system which is affected by a weak perturbation, it has been stated already in this paper that the linear response theory is a quite efficient method. However, it is not the case when the perturbation of a system is sufficiently large. In this case, besides the linear term, the other high order terms in the response function can also not be omitted. Consequently, the time propagation method becomes an effective one for simulating the nonlinear phenomenon.

Compared with the linear response theory, a remarkable drawback for the time propagation method is that it is very demanding on the computation. Hence, an efficient algorithm for the time propagation method becomes necessary for the practical application. It has been successfully shown in [**3, 4**] that the adaptive method can significantly improve the efficiency for the DFT calculations. It can also be expected that the adaptive method can improve the efficiency of algorithm for the time propagation TDDFT. Actually, some preliminary results in a forthcoming paper [**5**] have partially confirmed this.

In Section 1, a multi-physical model which combines the Maxwell equation and the TD-CDFT has been established, then the linear response theory has been introduced to solve this multi-physical model. It is worth mentioning that, like the time propagation method for TDDFT, a time domain solver the this coupled system can be used to study the nonlinear response when there is a strong EM field. Obviously, this solver consists of two parts. The first part is a time domain solver for the Maxwell equations. After the EM field is obtained, it is used as a vector field in the TD-CDFT to get the electron density and the current density with the second part, named, a time domain solver for the TD-CDFT. Based on our numerical experience, we think that the adaptive method can accelerate the numerical simulation of this multi-physical model. However, there are several numerical challenges. For example, one of these challenges is that how to efficiently combine the edge element for the Maxwell equation with the nodal element for the TD-CDFT. Another challenge is how to effectively design the indicator function (the monitor function) for the h-adaptive method (r-adaptive method). Since there are two different governing equations in the system, the regions of the singular solutions and/or the amplitudes of the singular solutions could be different. It is nontrivial to give a unified function to evaluate those singularities. We will try to propose a general time domain method for solving a coupled Maxwell-TDCDFT system in the future work.

References

[1] G. Bao, D. Liu and S. Luo, *A Multiscale Method for Optical Responses of Nano Structures*, submitted.

[2] G. Bao, D. Liu and S. Luo, *Multi-scale Modeling and Computation of Nano-Optical Responses*, submitted.

[3] G. Bao, G. Hu and D. Liu, *An h-adaptive finite element solver for the calculations of the electronic structures*, Journal of Computational Physics, 231, 4967-4979, 2012.
[4] G. Bao, G. Hu and D. Liu, *Numerical solution of the Kohn-Sham equation by Finite Element Methods with an adaptive mesh redistribution technique*, in minor revision.
[5] G. Bao, G. Hu and D. Liu, *An h-adaptive Finite Element solver to the Calculations of the Electronic Structures: Extension to the time-dependent case*, in preparation.
[6] C. Cohen-Tannoudji and J. Dupont-Roc and G. Grynberg, *Photons and Atoms: Introduction to Quantum Electrodynamics*, Wiley, New York, 1989.
[7] A. Stahl and I. Balslev, *Electrodynamics of the Semiconductor Band Edge*, Springer Tract in Mod. Phys. 110, Springer-Verlag, New York, 1987.
[8] O. Keller, *Local fields in the electrodynamics of mesoscopic media*, Phys. Rep., 268, 85-262, 1996.
[9] J. R. Chelikowsky, N. Troullier, and Y. Saad, *Finite-difference-pseudopotential method: Electronic structure calculations without a basis*, Phys. Rev. Lett., 72, 1240-1243, 1994.
[10] K. Cho, *Optical Response of Nanostructures: Microscopic Nonlocal Theory*, Springer, New York, 2003.
[11] D. E. Zhang, L. H. Shen, A. H. Zhou, and X. G. Gong, *Finite element method for solving KohnSham equations based on self-adaptive tetrahedral mesh*, Phys. Lett. A, 372, 5071-5076, 2008.
[12] X. Y. Dai, X. G. Gong, Z. Yang, D. E. Zhang, and A. H. Zhou, *Finite Volume Discretizations for Eigenvalue Problems with Applications to Electronic Structure Calculations*, Multiscale Modeling & Simulation, 9, 208-240, 2011.
[13] C. Yang, J. C. Meza, B. Lee, and L. W. Wang, *KSSOLV: a MATLAB Toolbox for Solving the Kohn-Sham Equations*, ACM Trans. Math. Software, 36, 1-35, 2009.
[14] T. Torsti, T. Eirola, J. Enkovaara, T. Hakala, P. Havu, V. Havu, T. Höynälänmaa, J. Ignatius, M. Lyly, I. Makkonen, T. T. Rantala, J. Ruokolainen, K. Ruotsalainen, E. Räs"anen, H. Saarikoski, and M. J. Puska. *Three real-space discretization techniques in electronic structure calculations*. Physica Status Solidi (b), 243, 1016–1053, 2006.
[15] J. E. Pask, and P. A. Sterne, *Finite element methods in ab initio electronic structure calculations*, Modelling Simul. Mater. Sci. Eng., 13, R71, 2005.
[16] E. Tsuchida, and M. Tsukada, *Adaptive finite-element method for electronic-structure calculations*, Phys. Rev. B, 54, 76027605, 1996.
[17] J. L. Fattebert, M. B. Nardelli, *Finite difference methods for ab initio electronic structure and quantum transport calculations of nanostructures*, Handbook of Numerical Analysis, 10, 571-612, 2003
[18] E. Runge and E. K. U. Gross, *Density-Functional Theory for Time-Dependent Systems*, Phys. Rev. Lett., 52, 997-1000, 1984.
[19] S. K. Ghosh and A. K. Dhara, *Density-functional theory of many-electron systems subjected to time-dependent electric and magnetic fields*, Phys. Rev. A, 38, 1149-1158, 1988.
[20] M. E. Casida, *Time-Dependent Density Functional Response Theory for Molecules*, In Recent advances in density functional methods; D. P. Chong, Ed. World Scientific, Singapore, 155-193, 1995.
[21] G. Vignale, *Current-Dependent Exchange-Correlation Potential for Dynamical Linear Response Theory*, Phys. Rev. Lett., 77, 2037-2040, 1996.
[22] P. Suryanarayana, K. Bhattacharya, and M. Ortiz, *A mesh-free convex approximation scheme for KohnSham density functional theory*, J. Comput. Phys., 230, 5226-5238, 2011.
[23] L. Lin, J. F. Lu, L. X. Ying, and W. N. E, *Adaptive local basis set for KohnSham density functional theory in a discontinuous Galerkin framework I: Total energy calculation*, J. Comput. Phys., 231, 2140-2154, 2012.
[24] M. van Faassen and P. L. de Boeij and R. van Leeuwen and J. A. Berger and J. G. Snijders, *Application of time-dependent current-density-functional theory to nonlocal exchange-correlation effects in polymers*, J. Chem. Phys., 118, 1044-1053, 2003.
[25] J. Ushida and K. Cho, *Dependence of Resonant SNOM Signal on Various Operation Modes*, Molecular Crystals and Liquid Crystals Science, 314, 215-220, 1998.
[26] A. Castro and H. Appel and M. Oliveira and C. A. Rozzi and X. Andrade and F. Lorenzen, and M. A. L. Marques, *octopus: a tool for the application of time-dependent density functional theory*, Phys. Stat. Sol. B, 243, 2465-2488, 2006.

[27] C. Fiolhais and F. Nogueira and M. A. L. Marques (Editors), *A Primer in Density functional Theory*, Lect. Notes Phys. 620, Springer-Verlag, New York, 2003.

[28] M. A. L. Marques and C. A. Ullrich and F. Nogueira and A. Rubio and K. Burke and E. K. U. Gross (Editors), *Time-Dependent Density Functional Theory*, Lect. Notes Phys. 706, Springer, Heidelberg, 2006.

Department of Mathematics, Michigan State University, East Lansing, MI 48824, and Department of Mathematics, Zhejiang University, Hangzhou 310027, China.
E-mail address: bao@math.msu.edu

Department of Mathematics, University of Macau, Macau, China.
E-mail address: hu@math.msu.edu

Department of Mathematics, Michigan State University, East Lansing, MI 48824.
E-mail address: richardl@math.msu.edu

Department of Mathematics, Iowa State University, Ames, IA 50011.
E-mail address: luos@iastate.edu